Advances in Geo-Energy Research

Vol. 21, No. 1, p. 42-59, 2026

Invited review

Mechanisms of deep coalbed methane occurrence: Review and perspectives

Sihao Li[1,2], Xin Li[1,2]*, Yong Tang[3], Yanpeng Chen[3], Jonathan A. Quaye[4], Chenlin Hu[1,2]*

[1]*School of Geology and Mining Engineering, Xinjiang University, Urumqi 830017, P. R. China*

[2]*Xinjiang Key Laboratory of Coalbed Methane Exploration and Development, Urumqi 830002, P. R. China*

[3]*Xinjiang Research Institute of Huairou Laboratory, Urumqi 830000, P. R. China*

[4]*Department of Petroleum Engineering, Kwame Nkrumah University of Science and Technology, Kumasi 451001, Ghana*

Keywords:
Deep coalbed methane
critical depth
occurrence mechanism
enrichment pattern
Langmuir equation
CO_2 sequestration

Cited as:
Li, S., Li, X., Tang, Y., Chen, Y., Quaye, J. A., Hu, C. Mechanisms of deep coalbed methane occurrence: Review and perspectives. Advances in Geo-Energy Research, 2026, 21(1): 42-59.
https://doi.org/10.46690/ager.2026.07.06

Abstract:
Deep coalbed methane occurs in geological settings characterized by high stress, high temperature, and high pressure, commonly referred to as "three-high" conditions. Owing to differences in genetic types, reservoir properties, and gas phases, its occurrence mechanisms differ substantially from those of shallow coalbed methane. Existing studies have generally reached a consensus on its occurrence boundaries and enrichment patterns. Based on an extensive literature review and representative cases from global basins, this review synthesized the genetic classifications, reservoir property evolution, coupled temperature-pressure-stress effects, hydrodynamic sealing conditions, and enrichment patterns of deep coalbed methane. A comprehensive formula for determining critical depth was proposed by integrating stress transition depth, adsorption capacity inflection point, and multiple geological parameters. This formula can be applied to regional-scale predictions and data-limited conditions. A coupled fracture-seepage-matrix-diffusion equation was established, and a revised productivity prediction model was developed. Existing evidence indicates that deep coalbed methane commonly forms through multistage hydrocarbon generation. It is dominated by thermogenic gas, with minor biogenic contributions. Gas mainly occurs in the adsorbed state, whereas the proportion of free gas increases with burial depth. Its enrichment is governed by structural style, cap rock sealing capacity, and fracture evolution. Critical depth indicators that were previously evaluated independently were integrated into a comprehensive multifactor criterion. The occurrence characteristics and migration behavior of deep coalbed methane were elucidated. The main controls on reservoir productivity were identified. These results provide theoretical support for efficient exploration and targeted exploitation of deep coalbed methane resources.

1. Introduction

Shallow and readily recoverable coalbed methane (CBM) resources have gradually declined in recent years. Therefore, deep CBM has emerged as a major focus of unconventional natural gas research and development owing to its considerable resource potential and broad development prospects (Wadsworth et al., 2002; Underschultz et al., 2016; Davydov, 2021) (Fig. 1). Deep CBM is mainly hosted in coal seams buried deeper than 1,500-2,000 m and is associated with complex geological conditions characterized by high stress, high temperature, and high pressure (Li et al., 2023; Lu et al., 2025). Research on deep CBM has progressed beyond traditional single adsorption-desorption models. Increasing attention is being paid to multiscale coupling mechanisms (Johnson and Flo-

*Corresponding author.
E-mail address: lsh6278@163.com (S. Li); lixinwaxj@xju.edu.cn (X. Li); tangyong_2026@163.com (Y. Tang); cyp2576@163.com (Y. Chen); jonathanatuquayequaye@gmail.com (J. A. Quaye); huchenlin@xju.edu.cn (C. Hu).
2207-9963 © The Author(s) 2026.
Received April 29, 2026; revised May 27, 2026; accepted June 16, 2026; available online June 20, 2026.

Yandy Scientific Press

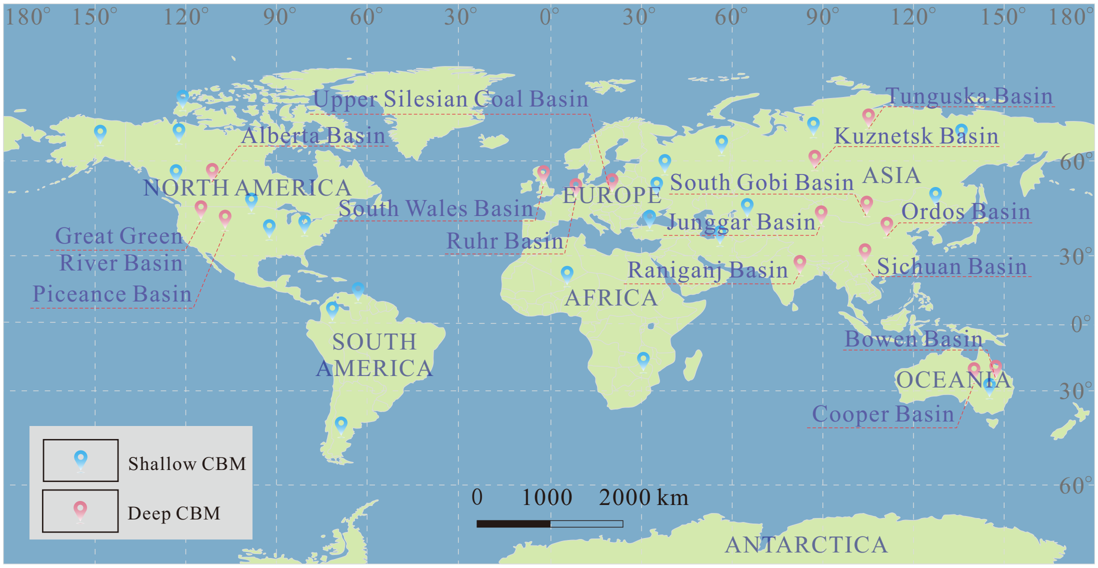

Fig. 1. Global distribution of shallow and deep CBM. The detailed data sources and corresponding references are listed in Table S1.

res, 1998; Wang et al., 2024; Hazra et al., 2025). Studies from the United States, Australia, China, and other countries have examined the effects of coal thermal evolution on hydrocarbon generation efficiency and gas-bearing capacity. These studies generally show that coal maturity, vitrinite reflectance, and pore structure evolution jointly control deep CBM occurrence and enrichment (Bustin et al., 2016; Underschultz et al., 2016; Li et al., 2025a). Tectonic stress regimes and their evolution also strongly affect reservoir permeability and fracture development (Ali Aghighi et al., 2024). Therefore, deep coal seams are highly heterogeneous in complex structural settings. This heterogeneity requires multi-basin comparisons and analyses of coupled geological processes to improve the understanding of occurrence mechanisms and support efficient deep CBM development.

Deep CBM differs significantly from shallow CBM in both reservoir properties and gas-bearing characteristics. This difference is mainly related to its "three-high" geological environment, which consists of high stress, high temperature, and high fluid pressure (Perera, 2018). In terms of reservoir properties, deep coal seams exhibit more complex pore structures. Adsorption pores may account for up to 78%, whereas shallow coals are dominated by exogenous seepage pores (Wang et al., 2024). Deep coal seams are denser, more intact, and less permeable (Wei et al., 2019). With increasing burial depth, both porosity and fracture density tend to decrease, making reservoir stimulation more difficult (Fu et al., 2024). Deep coals also commonly undergo more advanced thermal evolution, resulting in higher vitrinite content and greater coal strength. These features, combined with weak hydrodynamic conditions, favor the development of stable reservoir-seal assemblages (Wood and Sanei, 2016; Tian et al., 2019). However, under coupled high-temperature and high-pressure conditions, adsorption-desorption behavior becomes nonlinear. Therefore, both stress-enhanced gas adsorption and temperature-induced inhibition of adsorption should be considered (Zhou et al., 2020; Masum et al., 2023). With respect to gas-bearing characteristics, deep CBM generally occurs in saturated or supersaturated states and contains a higher proportion of free gas (Bannerjee et al., 2022). A "critical transition depth" is frequently observed, below which saturated adsorbed gas coexists with free gas (Zheng et al., 2019; Bannerjee et al., 2022; Kędzior and Teper, 2023). However, existing critical depth indicators are typically evaluated separately. However, a comprehensive quantitative framework that integrates these indicators has not yet been established. The mechanisms by which tectonic stress and fracture systems regulate gas enrichment across different evolutionary stages remain poorly understood. This limitation continues to hinder the systematic development of deep CBM accumulation models.

Previous reviews have provided valuable summaries of CBM genesis, reservoir characteristics, critical depth classifications, and development strategies (Moore, 2012; Qin et al., 2018; Li et al., 2023; Mohamed and Mehana, 2025). However, the relationships among critical depth determination, temperature-pressure-stress coupling, and gas occurrence mechanisms have not been comprehensively analyzed within an integrated framework. Therefore, a unified framework incorporating these key controls on deep CBM occurrence is still lacking.

This review examined global research progress on deep CBM occurrence mechanisms. The analysis covered genetic types, tectonic stress evolution, temperature-pressure conditions, hydrogeological parameters, and reservoir property evolution. It further synthesized enrichment patterns and controlling factors under different geological settings (Fig. 2). By integrating published studies with representative deep CBM case examples, this review identified the multivariable coupling controls on deep CBM occurrence and developed a comprehensive critical depth determination formula. Dual-field

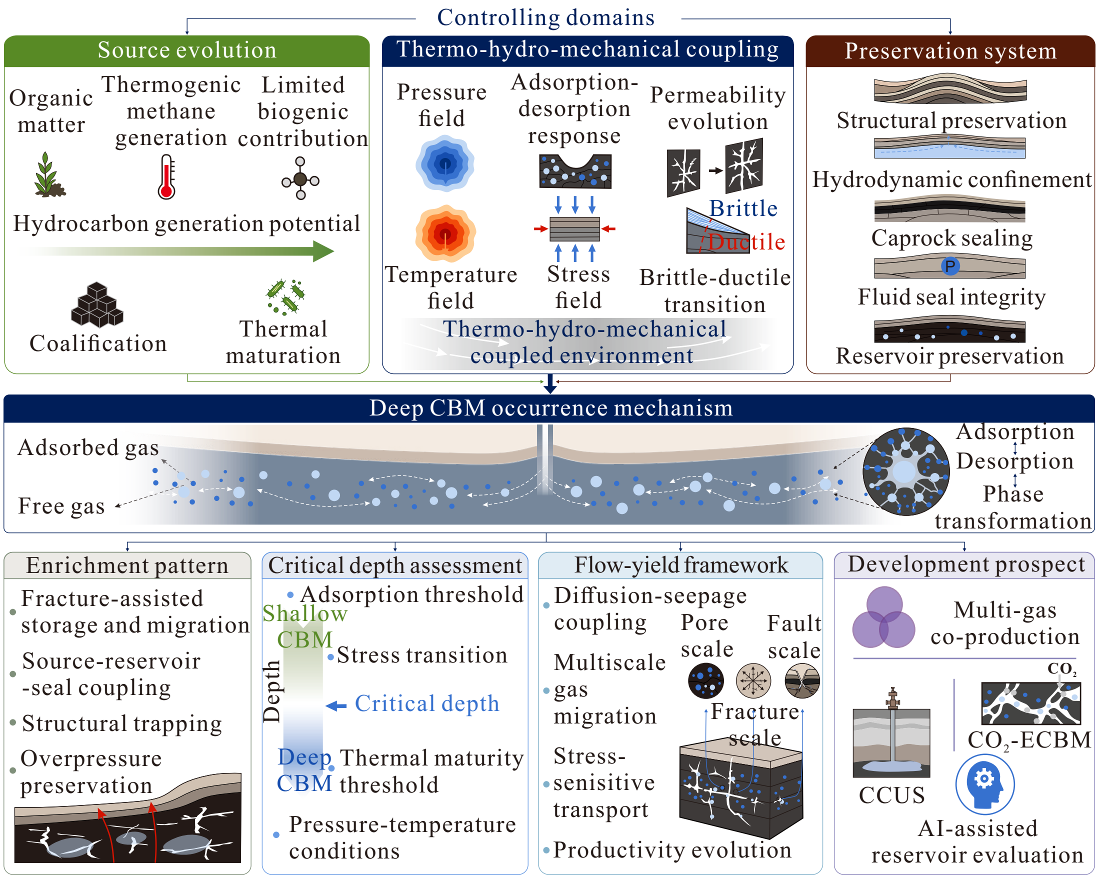

Fig. 2. Framework of the current research status and future development trends in deep CBM occurrence mechanisms.

coupling equations were constructed for migration analysis, and the productivity prediction formula was refined. These contributions provide a more comprehensive framework for understanding deep CBM occurrence and offer theoretical and practical support for resource assessment and efficient development.

2. Research progress

This section provides a systematic overview of the genetic mechanisms, key geological controls, enrichment patterns, and classification methods of deep CBM. It aims to clarify the mechanisms governing deep CBM occurrence within a multifactorial coupling framework.

2.1 Genetic analysis of deep CBM

2.1.1 Biogenic origin

Ocean Drilling Program investigations have identified evidence of microbial activity at 150 m below the seafloor (Oremland and Polcin, 1982; Whelan et al., 1986). Prokaryotic life has also been discovered in continental sedimentary rocks buried to depths of 2,800 m, indicating substantial biomass in the deep biosphere (Pedersen, 2000; Inagaki et al., 2015). Biogenic CBM has been reported in deep, low-rank coals from the Bowen Basin in Australia and the Ordos and Junggar Basins in China (Liu et al., 2022). Primary biogenic gas forms through microbial degradation of organic matter in near-surface coals. This process occurs under warm, neutral, low-salinity, and reducing conditions (Huang et al., 2017; Chen et al., 2023) (Eqs. (S1) and (S2)). Secondary biogenic gas develops in low-rank coals with vitrinite reflectance (R_o) $>$ 0.6% under the combined influence of microbial activity and groundwater. Its main sources are n-alkanes and mature organic matter (Huang et al., 2017; Kędzior and Teper, 2024) (Eq. (S3)).

2.1.2 Thermogenic origin

Thermogenic deep CBM originates from the thermal evolution of coal-forming organic matter. This pathway is the dominant gas generation mechanism in deep CBM systems. Mantle-derived gases introduced by deep magmatic activity or fault systems make only limited contributions. These inputs typically contain higher proportions of non-hydrocarbon gases than methane (CH_4) (Li et al., 2023). During metamorphism, organic matter undergoes successive deoxygenation and dehydrogenation. These reactions increase carbon content and generate substantial volumes of hydrocarbon gases, including CH_4, as well as non-hydrocarbon gases such as CO_2 and N_2 (Moore, 2012). The main gas generation stage corresponds to a vitrinite reflectance range of 0.6%-4.0%, which broadly covers the full CBM productivity window (Scott et al., 1994). The gas generation potential of deep coal seams is closely related to their degree of thermal evolution. Therefore, thermogenic gas can be further classified into two categories: Gas from therm-

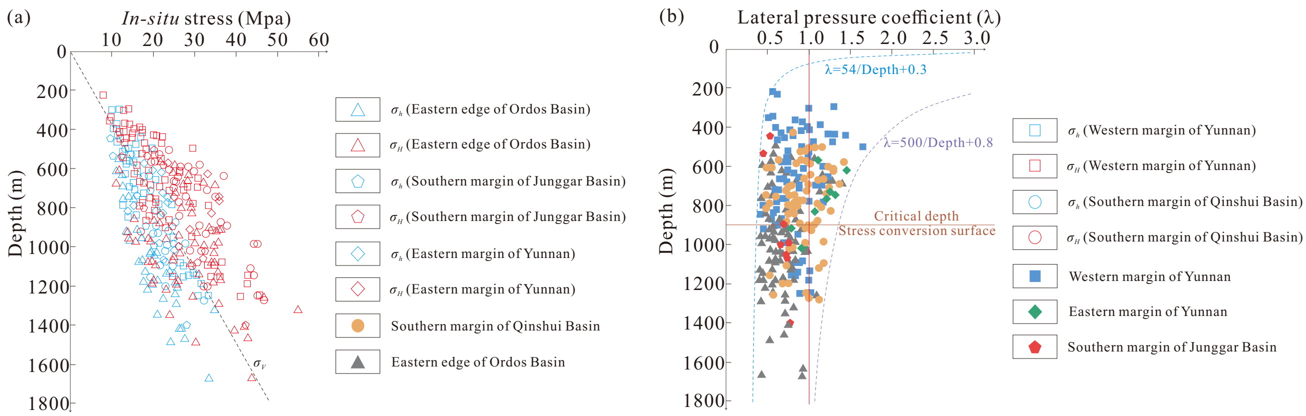

Fig. 3. Depth-dependent changes in (a) *in-situ* stress and (b) stress ratio in coal seams in China (modified from Li et al. (2023)). The symbols σ_h, σ_H, and σ_V denote the minimum horizontal, maximum horizontal, and vertical principal stresses, respectively.

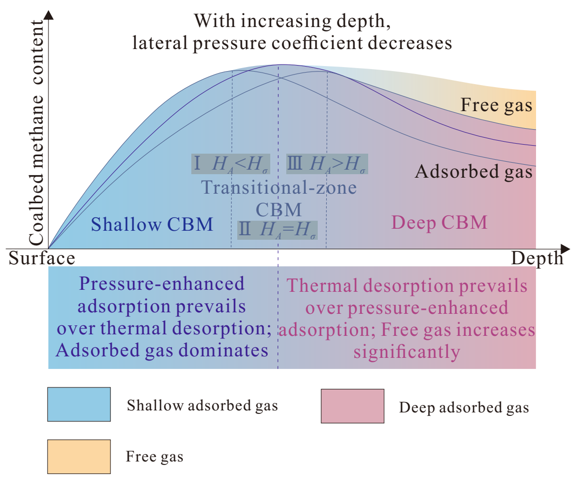

Fig. 4. Variation in CBM and total gas content with burial depth (modified from Chen et al. (2017) and Qin et al. (2018)). I: $H_A < H_\sigma$: A transition zone exists between deep and shallow CBM; and H_σ is the critical depth. II: $H_A = H_\sigma$: Coincide and jointly define the critical depth. III: $H_A > H_\sigma$: Same as Case I, a transition zone exists between deep and shallow CBM; HA is the critical depth.

al degradation and gas from thermal cracking (Song et al., 2012). Gas from thermal degradation forms during the evolution of medium-rank coals. It is mainly generated by cleavage of oxygen-containing functional groups and hydrocarbon side chains, producing CH_4 and heavier hydrocarbons (Eq. (S4)). In contrast, gas from thermal cracking forms during the evolution of high-rank coals, mainly through cracking of residual kerogen and liquid hydrocarbons (Bao et al., 2014; Zhang et al., 2025a) (Eq. (S5)).

2.2 Controlling factors of deep CBM

2.2.1 Tectonic stress evolution characteristics

The coupled effects of tectonic movement and the *in-situ* stress field are key controls on deep CBM occurrence (Ju et al., 2018; Fu et al., 2024). Tectonic structures, such as folds and faults, regulate the sealing capacity and permeability of coal reservoirs through extensional, compressional, and shear deformations (Ju et al., 2018). *In-situ* stress mainly acts on coal reservoir fractures and influences CBM occurrence by regulating coal seam permeability (Salmachi et al., 2021). Maximum horizontal stress, minimum horizontal stress, and vertical stress all increase with burial depth (Li et al., 2023) (Fig. 3(a)). *In-situ* stress magnitude is commonly described by the lateral pressure coefficient (λ), which represents the ratio of horizontal stress to vertical stress. This coefficient decreases as burial depth increases and follows a hyperbolic trend under the Hoek-Brown failure envelope (Chen et al., 2017). The stress transition surface ($\lambda = 1$) defines the critical stress depth. It marks the transition from horizontally dominated stress regimes in shallow coal seams to vertically dominated stress fields at greater depths (Rafiei Renani and Cai, 2022). Across this depth boundary, the dominant stress regimes change successively from reverse faulting to strike-slip and finally to normal faulting (Fig. 3(b)).

As burial depth increases, coal mechanical behavior shifts from brittle to ductile and exhibits more pronounced elasto-plastic characteristics. However, under normal faulting or extensional stress regimes, relatively brittle deep coals may still develop cleats and fractures. These structures facilitate gas accumulation and retention and contribute to the formation of stable CBM reservoirs (Sosnowski and Jelonek, 2022; Wang et al., 2023). In contrast, deep plastic coal seams under dominant vertical stress are more likely to undergo primary fracture closure, pore compression, and reservoir compaction. These processes significantly reduce permeability, thereby inhibiting CBM migration and enrichment (Tonnsen and Miskimins, 2010).

2.2.2 Coupled temperature-pressure effects on adsorption

The adsorption-desorption behavior of CH_4 in deep coal seams is governed by the thermodynamic coupling of temperature and pressure (Wu et al., 2016; Perera, 2018). Higher pressure favors CH_4 adsorption onto coal, whereas elevated temperature enhances molecular mobility. At greater burial depths, temperature becomes the main control on adsorbed gas content and promotes CBM desorption (Wu et al., 2016) (Fig. 4). This behavior is mainly related to interactions within deep coal seams. Interactions between micropore surfaces and

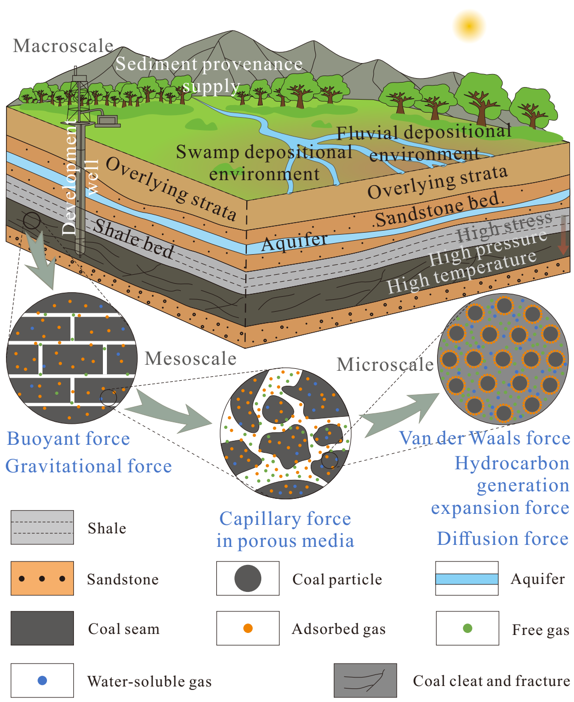

Fig. 5. Occurrence mechanism of deep CBM.

adsorbed gas molecules, as well as intermolecular interactions among gas molecules, are dominated by weak van der Waals forces (Li et al., 2025b). At elevated temperatures, gas molecules detach more readily from micropore surfaces (Wen et al., 2025).

Therefore, coal adsorption capacity initially increases with pressure and burial depth (Li et al., 2018). However, beyond a certain critical depth, elevated temperature reduces adsorption efficiency and produces a parabolic relationship between pressure and adsorption capacity. This trend favors the formation of highly saturated reservoirs and may contribute to supercritical fluid behavior in deep coal seams (Lu et al., 2025).

2.2.3 Hydrogeological confinement mechanisms

Restricted groundwater flow generally promotes CBM enrichment and preservation. In coal seams, CH_4 is stored in cleats, whereas water occurs in both cleats and matrix pores (Fig. 5). Hydrodynamic influence is mainly determined by the balance between hydrostatic pressure and pore pressure (Wood and Sanei, 2016; Liu et al., 2024). During the early stages of organic matter coalification, basin subsidence is slow, and original formation water occupies part of the pore space. Hydrostatic pressure is equal to pore pressure at this stage.

As burial depth increases, large volumes of CBM are generated and stored, causing pore pressure to gradually exceed hydrostatic pressure (Song et al., 2022). The increasing free gas volume displaces pore water and creates an overpressured environment favorable for deep CBM accumulation (Ji et al., 2026). During tectonic uplift of coal seams, groundwater may also reoccupy part of the pore space and form gas-water systems with varying saturation levels (Pang et al., 2021).

2.3 Enrichment patterns of deep CBM

Deep coal seams are generally characterized by high temperatures, high pressure, and high stress conditions. During coalification and subsequent tectonic evolution, they commonly develop complex pore-fracture systems (Wang et al., 2025). Strong gas-generation potential and effective CH_4 retention provide a material basis for deep CBM accumulation. Deep CBM enrichment is governed by the coupled effects of reservoir preservation, structural sealing, overpressure maintenance, multiscale pore fracture confinement, and the coexistence of adsorbed CH_4 and high-density free gas (Bannerjee et al., 2022; Sosnowski and Jelonek, 2022; Vasilenko et al., 2022).

2.3.1 Occurrence environment of deep CBM

The sedimentary environment determines the lithological assemblages of coal seams and overlying cap rocks. Deep coal deposits mainly form in continental and marine-continental transitional settings (Li et al., 2025a). Continental settings are dominated by fluvial, lacustrine, and swamp facies. In contrast, transitional environments commonly record multi-cycle sedimentation with interbedded coal seams, mudstones/shales, and sandstones (Xu et al., 2023; Wang et al., 2026) (Fig. 5). Lacustrine, deltaic, and neritic to shallow-marine mudrocks commonly serve as high-quality source rocks and cap rocks. Coal seams, tight sandstones, and mudstones/shales are typical cap rock types. These assemblages can be consistent with "self-sourcing and self-storage" and "source-below, reservoir-above" models (Tian et al., 2019). Continuous low-permeability cap rocks can suppress gas dissipation (Panwar et al., 2020). In cases where cap rocks also possess hydrocarbon-generating potential, relatively high localized accumulations may develop. For example, hydrocarbon-rich shale layers may serve as effective CBM cap rocks (Bannerjee et al., 2022; Kędzior and Teper, 2023; Yang et al., 2024). Where surrounding strata are enriched in sapropelic organic matter, coal seams may act as both reservoirs and seals (Li et al., 2022).

Tectonic processes govern reservoir formation and evolution. Faults, folds, and related structural deformations can facilitate gas migration and accumulation (Cao et al., 2018; Ghosh et al., 2022; Sosnowski and Jelonek, 2022; Zou et al., 2022). For example, in the Hangjinqi area of the Ordos Basin, tectonic uplift and pressure release have contributed to the development of natural gas reservoirs (Anees et al., 2022). Thermal anomalies can also influence coal reservoir characteristics. Magmatic upwelling during orogenic events may induce secondary hydrocarbon generation within coal seams, and igneous intrusions may positively influence reservoir properties (Hazra et al., 2025).

2.3.2 Occurrence conditions of deep CBM

Deep CBM is primarily stored in micropores, microfractures, kerogen, and coal matrix surfaces within thick coal seams. This mode of storage typically corresponds to a "self-sourcing and self-storage" reservoir system (Pajdak et al., 2019; Glatz et al., 2022; Lu et al., 2023) (Fig. 5). Except in exceptionally well-sealed coal seams, effective CBM accumulation requires that the volume of generated gas exceeds that lost through dissipation (Qin et al., 2018).

The occurrence of deep CBM is fundamentally controlled by the hierarchical pore-fracture system developed during coalification and subsequent geological evolution (Wei2019; Wang2025). Micropores (< 2 nm) contain abundant adsorption sites and have large specific surface areas. Therefore, they provide the principal storage domains for CH_4 retention in the coal matrix (Wang et al., 2023; Hazra et al., 2025). Mesopores (2-50 nm) provide transitional storage space and facilitate gas exchange between adsorption domains and larger flow pathways (Wang et al., 2024). Macropores (> 50 nm), cleats, and natural fractures provide effective pore volumes and interconnected transport networks. Therefore, they contribute to gas accumulation and migration (Ju et al., 2022; Wang et al., 2024; Yao et al., 2026) (Fig. 5). Under deep high-temperature and high-pressure conditions, these larger pore-fracture systems may accommodate substantial volumes of high-density free gas. This free-gas component is important for deep CBM occurrence and enrichment (Liu et al., 2022; Li et al., 2025a).

Deep CBM migration is characterized by pronounced multiscale transport. This process is governed by interactions among pore geometry, fluid properties, and effective stress (Ullah et al., 2022; Vasilenko et al., 2022). In nanopores and micropores, molecular diffusion, as described by Fick's law, remains an important transport mechanism (Ren et al., 2021). When the pore diameter approaches the molecular mean free path, the confinement effects become increasingly significant. Under these conditions, Knudsen diffusion may contribute substantially to gas transport (Mostafa et al., 2023; Guang et al., 2026). CH_4 adsorbed on pore surfaces can also migrate via surface diffusion. This process is an important mass transfer mechanism in organic matter-rich domains with large specific surface areas (Yang et al., 2026). As gas moves from nanopores to mesopores and macropores, pore wall interactions gradually weaken, and slip-flow behavior may develop (Xiao et al., 2025). In connected cleat and fracture systems, pressure-driven seepage governed by Darcy's law becomes the dominant transport mechanism (Ren et al., 2021) (Fig. 5). Permeability evolution in deep CBM reservoirs is also strongly stress-sensitive because fracture conductivity is closely coupled with effective stress variations, causing dynamic changes in the fracture aperture and flow capacity (Wang et al., 2024; Yao et al., 2026).

Overall, deep CBM enrichment reflects a systematic transition in CH_4 occurrence, preservation, and transport mechanisms with increasing burial depth. CH_4 storage changes from adsorption-dominated conditions to a dual-storage system of adsorbed and free gas. The main controls on enrichment also shift from gas generation and adsorption capacity to pressure preservation and stress-constrained sealing efficiency. CH_4 migration changes from a fracture-dominated flow to multi-scale coupled transport. Collectively, these changes define the distinctive enrichment pattern of deep CBM and fundamentally distinguish it from shallow CBM systems.

2.4 Classification of deep CBM

2.4.1 Critical depth of deep CBM

Critical depth serves as a key parameter for distinguishing shallow CBM from deep CBM. As coal exploration and development move toward deeper seams, the depth definition of "deep" differs among countries (Table S1). In China, technological constraints have led to an adjustment of the depth criterion from 1,000 to 2,000 m, whereas international standards generally range from 1,500 to 3,000 m (Li et al., 2023). Geologically, critical depth is governed by the combined effects of temperature, pressure, and *in-situ* stress evolution. With increasing burial depth, temperature (2.5-3.5 °C/100 m) and pressure (~ 1.0 MPa/100 m) generally increase in an approximately linear manner. During early burial, elevated pressure promotes CH_4 adsorption and progressively increases adsorbed gas content. After a certain threshold is exceeded, increasing temperature and compaction reduces micropore volume and adsorption capacity. Therefore, free gas gradually becomes the dominant phase (Qin et al., 2018). The depth corresponding to the inflection point in the adsorbed gas content is defined as the adsorption critical depth (H_A). A stress critical depth (H_σ) also exists and marks the transition from horizontal to vertical stress dominance within the stress field (Li et al., 2023). If these two depth boundaries differ, an intermediate transition zone may develop between mid-depth and deep coal seams (Zheng et al., 2019; Li et al., 2023) (Fig. 4). Because sedimentary evolution and tectonic regimes differ among basins, critical depth is regionally variable rather than universally fixed. Therefore, a combined analysis of H_A and H_σ is required. By integrating adsorption, stress, and burial-related characteristics, this approach provides a more reliable basis for identifying the critical depth of deep CBM.

2.4.2 Occurrence phases of deep CBM

Deep CBM mainly occurs as adsorbed and free gas, with a minor fraction dissolved in formation water (Moore, 2012; Tamamura et al., 2020). Increasing burial depth and temperature reduce CH_4 adsorption capacity through micropore thermal expansion and intensified molecular motion. After adsorption saturation is reached, gas begins to desorb as free gas, particularly in fracture-rich zones (Ji et al., 2026). Under the elevated temperature and pressure conditions of deep reservoirs, CH_4 can enter a supercritical state. This phase differs physically from conventional gas (Wu et al., 2016). Recent pressure-maintaining coring and *in-situ* gas desorption experiments have improved the quantification of in-place gas phase distribution in deep coal seams. They also reduce the underestimation of free gas content caused by degassing during conventional sampling (Huang et al., 2023). Carbon and hydrogen isotope analyses of adsorbed and free CH_4 have further revealed distinctive isotopic fractionation patterns. These patterns indicate adsorption-desorption equilibrium and diffusive migration and provide insights into gas-phase partitioning mechanisms at depth (Wu et al., 2025). If adsorption sites remain unsaturated, free gas can be re-adsorbed (Mudoi et al., 2022). CH_4 dissolved in formation water can be released as free gas during pressure reduction or re-dissolved under

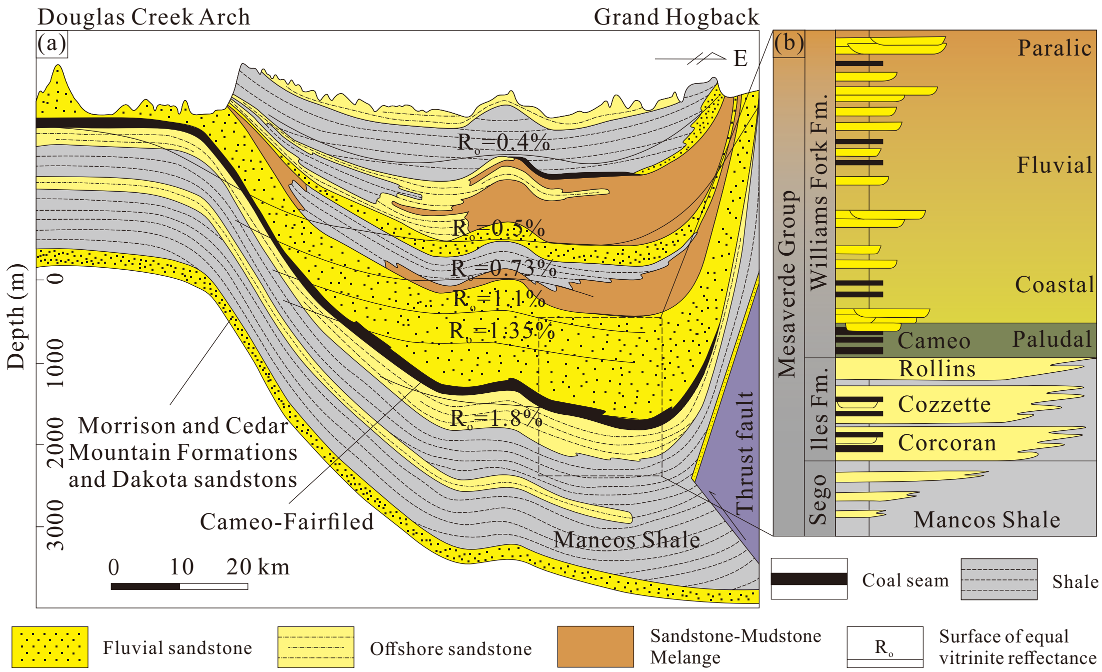

Fig. 6. Lithological profile and sedimentary facies of the central Piceance Basin, USA (Stroker et al., 2013): (a) Lithological profile of the central Piceance Basin and (b) Sedimentary facies of the Mesaverde Group.

high-pressure and low-temperature conditions. Transformation between adsorbed and dissolved phases mainly occurs via diffusion (Tamamura et al., 2020). These phase transitions are governed by the dynamic interplay among temperature-pressure conditions, stress regimes, hydrodynamics, and pore structures. This interplay ultimately constrains CBM distribution and recoverability (Mohanty and Pal, 2017; He et al., 2025).

2.4.3 Gas-bearing systems in deep coal seams

Deep coal seams can be classified into wet and dry CBM systems based on their water content. Wet systems commonly contain micropores and mesopores that retain immobile capillary water or bound water. Macropores may also become saturated by surface water intrusion, particularly along uplifted basin margins (Wang et al., 2021). In contrast, dry systems are generally characterized by macropores from which water is more readily expelled (Liu et al., 2024). Deep coal seams with high hydrocarbon generation potential are commonly overpressured and exhibit elevated free gas content. When gas pressure exceeds hydrostatic pressure, pore water is displaced, and a dry system favorable for production is formed (Fall et al., 2012; Liu et al., 2024). Dry CBM systems typically support gas production without dewatering or pressure reduction, as demonstrated in the northern San Juan Basin in the United States. Such overpressured dry reservoirs are regarded as "sweet spots" for deep CBM development (Scott et al., 1994; Li et al., 2025b).

3. Typical examples

Global basins vary in geological structure, thermal maturity, and coal rank. These differences produce regional variations in the mechanisms that control deep CBM accumulation. Despite these differences, a common feature is the synergistic control exerted by thermodynamic conditions and reservoir properties. This section analyzes representative basins in terms of geological evolution, burial depth, temperature-pressure regimes, and reservoir characteristics to clarify the dominant controls on deep CBM occurrence.

3.1 Piceance Basin, USA

The Piceance Basin was the first region to achieve major advances in deep CBM production through the combined development of deep coal seams and tight sandstones. It formed during the Laramide orogeny and dips westward with a steeper eastern margin (Johnson, 1989). From the Late Cretaceous to the Tertiary, rapid subsidence produced thick accumulations of marine and non-marine clastic sediments. The main coal seams occur in the Williams Fork Formation of the Mesaverde Group. Within this formation, the basal Cameo-Fairfield coal zone represents the principal producing interval (Fall et al., 2012; Coe et al., 2024) (Fig. 6). As burial depth increases, coal rank progresses from lignite to medium-volatile and high-volatile bituminous coal. This rank progression is accompanied by a significant increase in gas content (Stroker et al., 2013; Bustin et al., 2016; Eberle et al., 2024) (Fig. 6).

Regional temperatures often exceed 75 °C, the upper threshold for methanogenic microbial activity. Overpressured conditions facilitate CH_4 migration and enrichment from underlying organic-rich shales into coal seams (Johnson and Flores, 1998; Stroker et al., 2013). Low-permeability tight sandstones overlying coal seams promote natural fracturing and partial CH_4 migration. These processes form secondary tight sandstone gas reservoirs (Cumella and Scheevel, 2008).

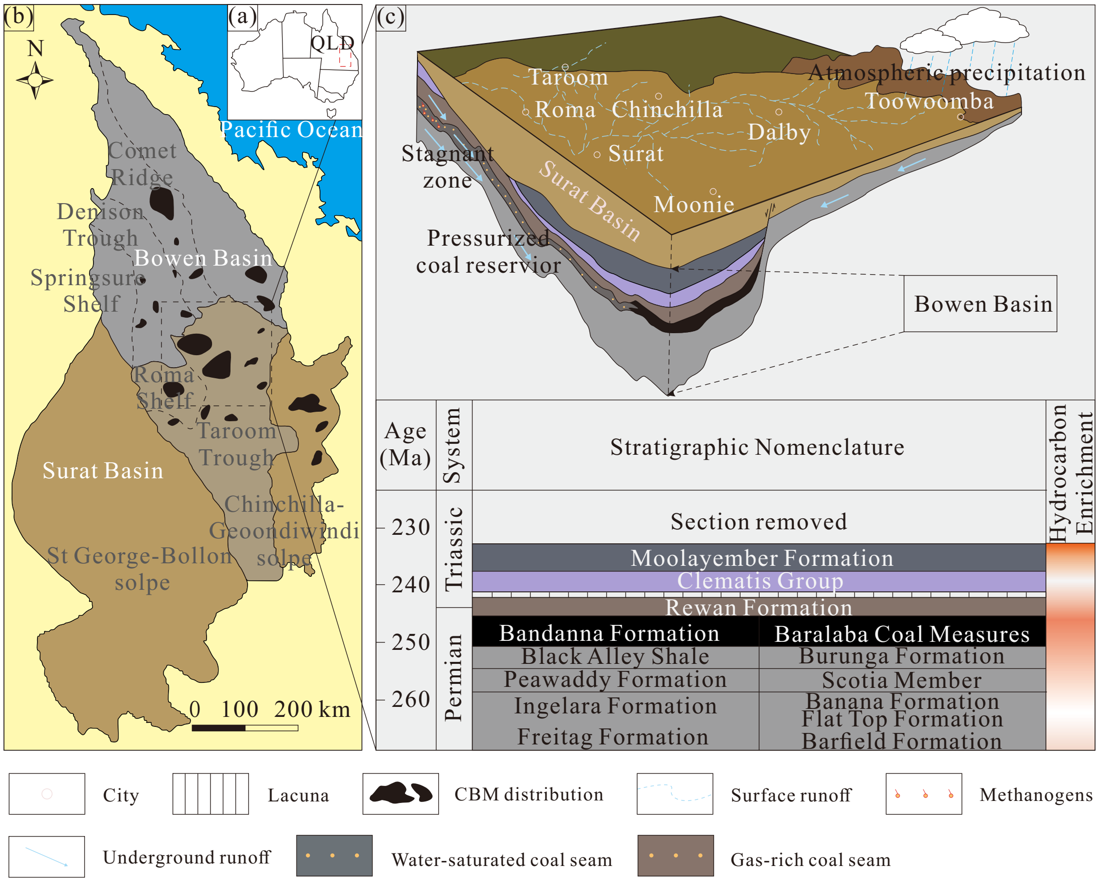

Fig. 7. Resource potential controls of CBM in the Bowen Basin, Australia: (a) Location of the Bowen Basin (Brakel et al., 2009), (b) CBM resource distribution in the Bowen Basin (modified from Li et al. (2014) and Towler et al. (2016)) and (c) burial model of the Bandanna coal seam in the Blackwater Group, Bowen Basin (modified from Towler et al. (2016); Pandey et al. (2021); Ali Aghighi et al. (2024)).

3.2 Bowen Basin, Australia

The Bowen Basin in Queensland, Australia, is a foreland basin formed in a back-arc setting (Fig. 7(a)). The basin developed a westward-dipping geometry under east-west compression, accompanied by thrust faults along the basin axis (Sahlström et al., 2018; Asmussen et al., 2023) (Fig. 7(b)). The primary coal-bearing strata belong to the Permian Bandanna Formation, which was deposited in a deltaic swamp environment (Li et al., 2014; Towler et al., 2016). The coals are vitrinite-rich, with R_o values of 0.69%-0.97%, and are classified as Type II-III medium-rank bituminous coals (Freij-Ayoub, 2012; Cui et al., 2025). Despite the low geothermal gradients in the Taroom Trough, an Early Triassic thermal event triggered rapid coal maturation and gas generation (Golding et al., 1999; Hamilton et al., 2020; Everts et al., 2024). Tensile stress at the anticlinal axes promotes fracture development. Fracture orientations further indicate upward gas migration pathways (Salmachi et al., 2021; Rajabi et al., 2024). In some areas, weak groundwater flow zones coincide with groundwater flow direction and bedding dip. These conditions favor methanogen activity and biogenic gas generation (Huang et al., 2017) (Fig. 7(c)). As burial depth increases, effective stress intensifies, causing fracture closure and permeability reduction. This process contributes to CBM preservation (Ali Aghighi et al., 2024).

3.3 Ordos Basin, China

The Ordos Basin in north-central China is a typical multicentric cratonic basin (Li et al., 2018; Zhao et al., 2024b) (Fig. 8(a)). In the Daning-Jixian area, deep CBM mainly occurs in the Carboniferous-Permian coal-bearing strata (Fig. 8(b)). Vitrinite reflectance (R_o) ranges from 1.37% to 3.40%, indicating medium- to high-rank coal (Wang et al., 2026). The Permian strata are characterized by marine-continental transitional facies and are subdivided into the Shanxi, Taiyuan, and Benxi formations (Wang et al., 2023). The Shanxi Formation primarily consists of deltaic deposits. In contrast, the Taiyuan and Benxi formations include deltaic, lagoonal, tidal flat, and shallow-marine shelf sediments (Yan et al., 2023) (Fig. 8(c)). The Benxi Formation hosts stable and thick primary coal seams. These coal seams are rich in nanopores and microfractures, which favor deep CBM accumulation (Yao et al., 2026).

Organic matter experienced dual-stage hydrocarbon generation during Triassic burial metamorphism and subsequent Cretaceous magmatic thermal events. This dual-stage hydro-

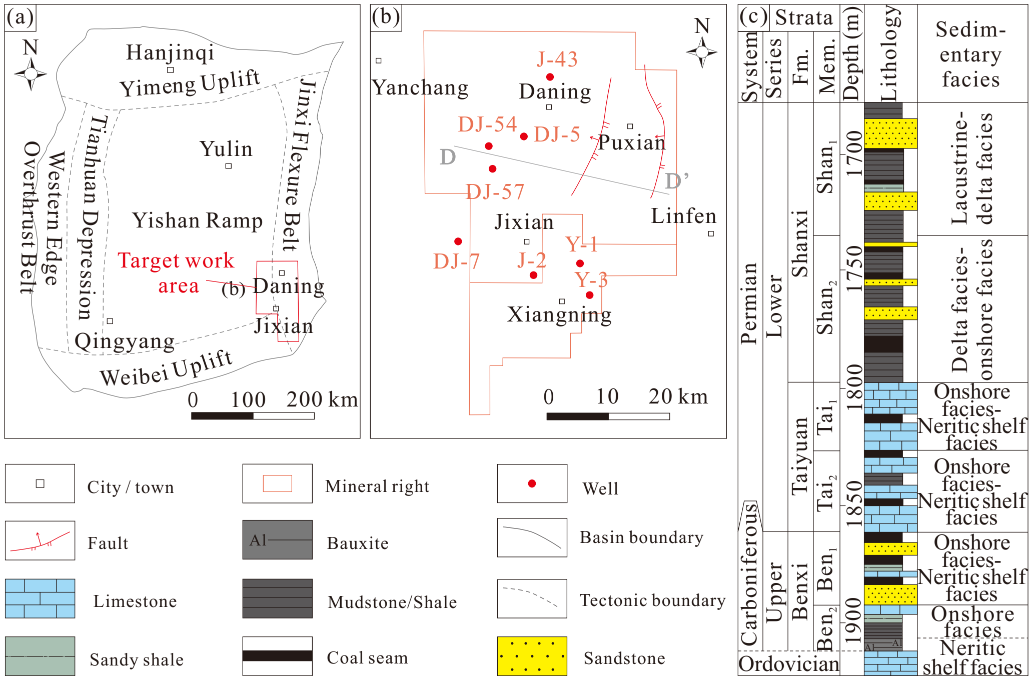

Fig. 8. Geological setting of the Daning-Jixian area, Ordos Basin, China (Wang et al., 2024): (a) Location of the study area within the Ordos Basin, (b) well distribution (cross-section DD' is shown in Fig. 9) and (c) stratigraphic column of the study area.

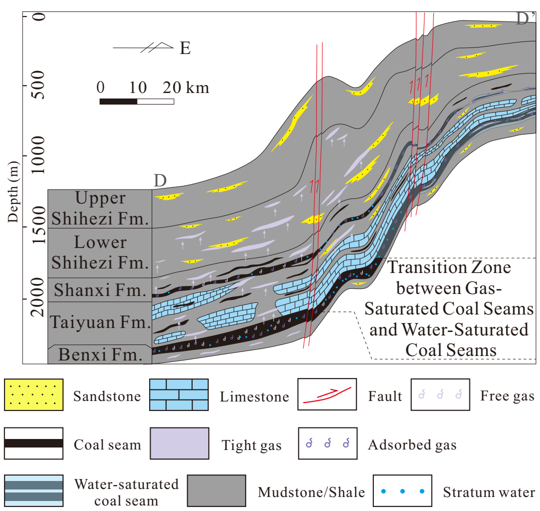

Fig. 9. Geological profile of the gas-bearing Carboniferous-Permian strata in the Daning-Jixian area, Ordos Basin, China (Li et al., 2025a). The location of cross-section DD' is illustrated in Fig. 8(b).

carbon generation was accompanied by well-developed fracture systems (Yan et al., 2023). Overlying marine limestones and interbedded marls can form excellent cap rocks (Fig. 9). Meanwhile, both adsorbed and free gas contents increase significantly with burial depth and geothermal gradient (Li et al., 2025a).

4. Discussion

Large-scale commercial production of deep CBM has been achieved in several regions. However, global development remains limited by the inherent instability of deep CBM systems and the high cost of resource extraction (Table S2). This section discusses recent advances in the understanding of deep CBM accumulation mechanisms and reviews the current status of exploration and development. It further compares previous studies to identify research gaps and potential future directions.

4.1 Development trends

4.1.1 Critical depth and temperature-pressure conditions

In deep coal seams, a transition in CBM occurrence characteristics typically occurs near a critical depth. This depth represents a key boundary governed by the coupled evolution of temperature and pressure (Li et al., 2023). As burial depth increases, geothermal and pressure gradients steepen significantly. These changes alter coal matrix structure, pore characteristics, and stress response behavior (Rafiei Renani and Cai, 2022; Li et al., 2023). Adsorbed gas remains the dominant phase, but increasing thermal maturity, tectonic compaction, and *in-situ* stress progressively modify reservoir permeability, gas occurrence mechanisms, and productivity response patterns (Chen et al., 2017; Rajabi et al., 2024). Therefore, critical depth marks a systematic shift in coal reservoir properties. It also provides a key reference for production optimization, including productivity evaluation, fracturing intensity design, and well pattern deployment (Tambaria et al., 2022; Mohamed and Mehana, 2025). Building on previous studies, this review integrated multiple controlling factors, including geothermal gradient, formation pressure, *in-situ* stress field, coal rock strength, and thermal maturity. These controls were used to establish a quantitative formula for characterizing the critical depth of deep CBM with potential global applicability. The formula is expressed as follows:

$$H_c = \max\left(H_\sigma,\ H_A,\ \alpha\frac{S_T}{T_g} + \beta\frac{S_P}{P_g} + \gamma\frac{\sigma_H}{\sigma_v} + \delta\frac{\sigma_v}{\sigma_v} + \varepsilon(R_o - R'_o)\right) \tag{1}$$

where H_c is the critical depth; H_σ is the depth marking the transition from horizontal to vertical stress dominance; H_A is the inflection depth of adsorbed gas content; S_T is the temperature threshold; T_g is the geothermal gradient; S_P is the pressure threshold; P_g is the pressure gradient; σ_H is the maximum horizontal stress; σ_V is the vertical principal stress; σ_c is the coal rock strength; R_o is the vitrinite reflectance; R'_o is the critical maturity for CH_4 generation; and $\alpha - \varepsilon$ are the weighting coefficients assigned to each parameter. Because these mechanisms do not necessarily occur at identical depths, the maximum value among them is considered to define the critical depth at which all required deep conditions coexist.

4.1.2 Variations in physical properties of coal reservoirs

As burial depth increases, the physical properties of coal reservoirs change substantially. These changes favor the formation of saturated or even supersaturated CBM reservoirs and increase the proportion of free gas (Kang et al., 2023; Li et al., 2023). However, deep reservoirs commonly undergo pore compaction, permeability reduction, and fracture closure. These processes hinder gas migration (Tonnsen and Miskimins, 2010; Liu et al., 2024). Coal matrix hardening results from increased vitrinite content and skeletal reinforcement. This hardening contributes to micron-scale pore compaction. Meanwhile, primary fracture connectivity is largely constrained by the prevailing *in-situ* stress field (Chelgani et al., 2024). Therefore, deep coal reservoirs have much lower pore connectivity than shallow coal seams. Young's modulus and Poisson's ratio also increase nonlinearly with depth (Tonnsen and Miskimins, 2010; Zheng et al., 2019). Under these temperature-pressure conditions, adsorption behavior becomes increasingly complex and is strongly coupled with pore deformation and temperature-driven desorption (He et al., 2025). Elevated temperature weakens adsorption capacity by expanding micropores and accelerating molecular mobility. In contrast, high pressure enhances gas densification and promotes multilayer adsorption within nanopores (Huang et al., 2026). These physical changes limit the natural CBM storage capacity of deep coal seams and increase the demand for hydraulic fracturing and reservoir stimulation.

4.1.3 Tectonic and *in-situ* stress control mechanisms

In deep CBM systems, coal gas-bearing capacity is not controlled solely by tectonic deformation or a single stress regime. It is jointly influenced by structural configuration, stress evolution trajectory, and mechanical response of coal (Ghosh et al., 2022; Rajabi et al., 2024). Tectonic movements define the initial geometry and fracture architecture of coal seams. Stress fields then dynamically regulate the functions of these structures. They determine whether the structures become effective seepage pathways or sealing barriers (He et al., 2017; Salmachi et al., 2021). Current studies have confirmed that the critical stress depth defines the transformation among principal stress types. However, further evidence indicates that this transformation is gradual, rather than abrupt. A transitional zone with progressively varying stress states often develops near the critical depth (Ju et al., 2022; Lv et al., 2025). In this zone, stress conditions are strongly coupled with the brittle-ductile transformation of coal rocks. This coupling establishes a "fracture regeneration window" that plays a critical role in CBM migration (Fu et al., 2024; Zhao et al., 2024b). Different structural and stress regime combinations produce different coal occurrence patterns. For instance, in thrust-shear or fold zones, brittle-ductile transitional coals with high vitrinite contents commonly develop tensile-shear fractures. These fractures provide effective gas-bearing spaces. In contrast, under compressional conditions, plastic deformation commonly causes fracture closure (Ju et al., 2022; Fu et al., 2024). Therefore, the microstructural evolution of coal rocks under tectonic stress should be examined carefully to address the "gas-rich but low-yield" phenomenon.

4.2 Prospects for deep CBM development

Coal-bearing strata are widely distributed worldwide. In transitional marine-terrestrial facies, repeated sedimentary cycles generate interbedded coal seams, shales, and tight sandstones. These strata commonly have rich organic content and favorable source-reservoir-cap combinations (Cao et al., 2019; Lv et al., 2020). Therefore, CBM, shale gas, and tight gas commonly coexist and are co-stored (Li et al., 2021). CBM productivity depends on both gas occurrence conditions and extraction technologies. Gas occurrence conditions determine gas content, and extraction technologies control actual output (Johnson and Flores, 1998; Xu et al., 2023) (Table S2). Co-exploitation of multiple gas resources can substantially enhance single-well production and reduce drilling costs (Fig. 10). For instance, in the Piceance Basin of the United States, the combined development of deep coal seams and tight sandstones has achieved favorable production. In the Qinshui Basin of China, gas coexistence has also been identified in the Shanxi and Taiyuan formations. However, independent exploitation of shale gas or tight gas poses a higher technical risk (Zhang et al., 2025b). Multi-gas co-production may also increase the compositional complexity and risk of hazardous gas emissions.

Deep coal seams typically exhibit elastoplastic behavior. Therefore, conventional CBM and shale gas fracturing techniques are often ineffective. Stimulation methods capable of relieving stress on a large scale while utilizing gas adsorption and shrinkage effects are required (Dunlop et al., 2017). Several stimulation technologies have been proposed for deep coal reservoirs. Optimized hydraulic fracturing remains the most widely used method. It improves reservoir connectivity by generating complex fracture networks (Salmachi et al., 2021; Lu et al., 2023). Liquid CO_2 fracturing has received increasing attention because phase transition expansion and cryogenic effects can promote fracture propagation and reduce water-related damage (Lu et al., 2023). Liquid nitrogen fracturing

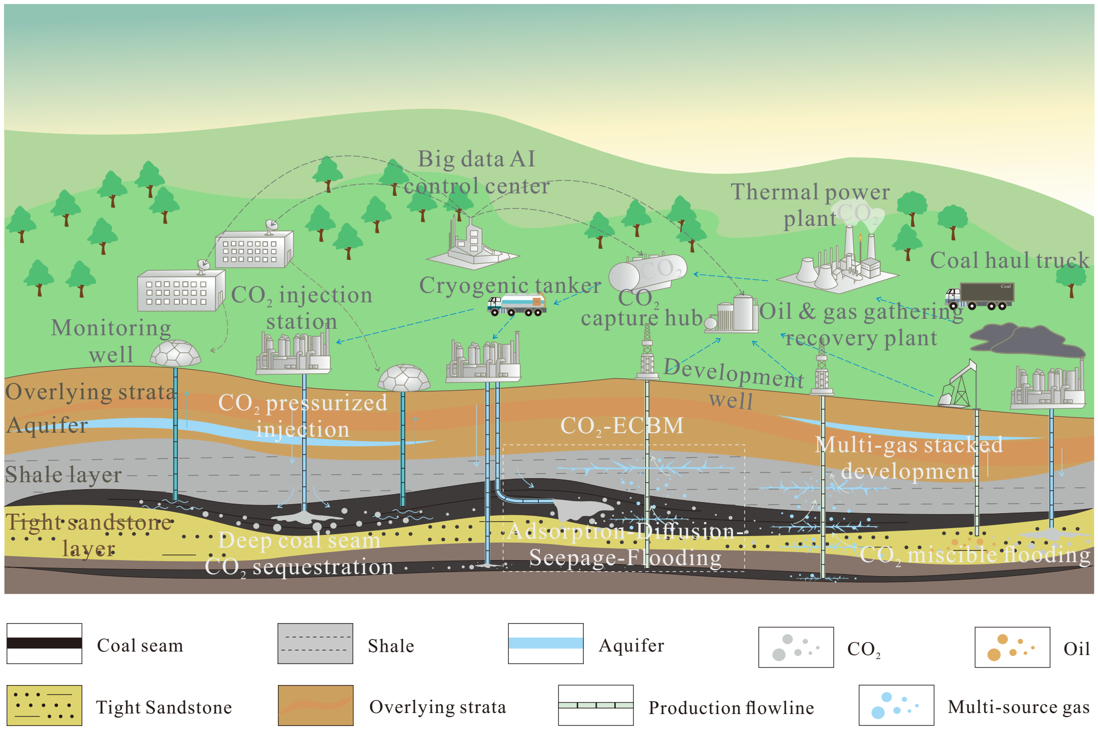

Fig. 10. Development prospects of deep CBM.

enhances permeability via thermal shock-induced cracking and freeze-thaw damage. This method is particularly suitable for water-sensitive coal seams (Longinos et al., 2025). Thermal stimulation, including heat injection, microwave heating, and electrical heating, can enhance CH_4 desorption and diffusion by modifying adsorption equilibrium and matrix transport properties (Li et al., 2026). These technologies have shown encouraging results. However, their effectiveness remains strongly influenced by reservoir depth, stress conditions, coal properties, and operational constraints. Carbon capture, utilization, and storage (CCUS) technologies provide an additional pathway for simultaneous CH_4 recovery and carbon sequestration (Lee et al., 2016; Jiang and Ashworth, 2021; Welsby et al., 2021). CO_2 sequestration is the terminal step in the CCUS chain, and deep unmineable coal seams are often used as target formations (Jiang et al., 2022) (Fig. 10). Coal has a high adsorption affinity for CO_2, providing a theoretical basis for CO_2-enhanced CBM (CO_2-ECBM) recovery and geological sequestration (Tambaria et al., 2022; Liu et al., 2022). Middle- to high-rank coals generally adsorb approximately twice as much CO_2 as CH_4. Therefore, injected CO_2, particularly under supercritical conditions, can preferentially occupy adsorption sites and displace CH_4 from the coal matrix (Mwakipunda et al., 2023; Govindarajan et al., 2025; Hu et al., 2026). However, CO_2 injection alters reservoir properties through coupled adsorption-deformation processes (Zou et al., 2026). CO_2 adsorption may induce coal matrix swelling, whereas CH_4 desorption may cause matrix shrinkage (Mukherjee and Misra, 2018). Competition between swelling and shrinkage, along with stress-dependent permeability evolution, can significantly modify fracture conductivity, injectivity, and CH_4 recovery efficiency (Sampath et al., 2017; Asif et al., 2024). Therefore, the effectiveness of CO_2-ECBM and geological storage depends on the coupled effects of adsorption behavior and permeability evolution during CO_2 injection. For CO_2 injection, the system should be modeled using the two-phase Darcy's law. Following the oil-water analyses of Wang et al. (2023), this formulation can be applied to gas-water flow modeling:

$$v_{gas} = -\frac{kk_{rg}}{\mu_g}\nabla P \tag{2}$$

$$v_{water} = -\frac{kk_{rw}}{\mu_w}\nabla P \tag{3}$$

where v_{gas} is the gas seepage velocity; v_{water} is the water seepage velocity; k_{rg} is the gas relative permeability; k_{rw} is the water relative permeability; ∇P is the pressure gradient; and μ is the gas viscosity.

Owing to the multiscale transport behavior of deep coal reservoirs, CH_4 migration involves both matrix diffusion and fracture seepage. Therefore, a dual-field coupled model integrating Fickian diffusion and Darcy flow was established to characterize the matrix diffusion-fracture flow process:

$$\frac{\partial}{\partial t}\left[\phi_m C_m + \rho_s(1-\phi_m)\rho_a + \phi_f \rho_g\right] = \nabla\cdot\left(D_m \nabla C_m - \frac{k_f}{\mu}\rho_g \nabla P\right) \tag{4}$$

where ϕ_m is the coal-matrix porosity; C_m is the matrix free-gas concentration; ρ_s is the coal particle density; ρ_a is the adsorbed gas concentration; ϕ_f is the effective free-gas porosity; ρ_g is the free-gas density in fractures; D_m is the effective matrix diffusion coefficient; k_f is the fracture permeability; μ is the gas viscosity; and P is the fracture network pressure.

Field demonstrations in the San Juan Basin (United States), Qinshui Basin (China), Ishikari Coalfield (Japan), and several other coal-bearing basins have confirmed the technical feasibility of deep CBM development and CO_2-enhanced recovery under suitable geological conditions (Godec et al., 2014; Mukherjee and Misra, 2018; Asif et al., 2022). However, deep coal seams commonly exhibit low mechanical strength and stress-sensitive fracture systems. These features may significantly affect CO_2 containment and storage performance. Therefore, further investigation of CO_2 occurrence mechanisms, migration processes, and long-term sequestration security is required.

In conventional CBM production, each stage requires manual evaluation and parameter adjustment. This workflow results in long development cycles, high operational costs, low efficiency, and elevated risk levels (Mohamed and Mehana, 2025). Existing adsorption isotherm models, such as the Freundlich, BET, and Dubinin-Radushkevich equations, describe different adsorption characteristics. However, the Langmuir equation remains the most widely applied model because of its simplicity and practical applicability. CBM reserves can be estimated more effectively by modifying the Langmuir equation and adjusting its parameters for different gas-bearing systems (Langmuir, 1918; Yang et al., 2019; Mohamed and Mehana, 2025; Eq. (5)). Because gas desorption in deep coal seams is controlled by the effective pressure difference during drainage, the reservoir pressure term is replaced with the net driving pressure (P_n). The modified Langmuir adsorption equation is expressed as:

$$Q_L = V_L \frac{P_n}{P_L + P_n} \tag{5}$$

where Q_L is the modified Langmuir adsorption capacity; V_L is the Langmuir volume; P_n is the net driving pressure; and P_L is the Langmuir pressure.

According to Eq. (5), the effective gas production potential of deep CBM reservoirs consists of adsorbed gas and free gas. CH_4 is primarily retained in the coal matrix, whereas gas migration occurs through the fracture system. Therefore, the permeability contrast between matrix permeability and fracture permeability is introduced to characterize matrix-to-fracture gas migration efficiency (Moore, 2012; Mostafa et al., 2023). Considering its nonlinear influence, the permeability ratio is expressed in logarithmic form. During reservoir depletion, increasing effective stress reduces fracture conductivity and gas deliverability (Fu et al., 2024; Xiao et al., 2025) (Eqs. (6)-(8)). This stress sensitivity is represented by an exponential attenuation term. Therefore, the adsorbed gas term can be expressed as:

$$Q_a = Q_L \left(1 + \ln \frac{k_f}{k_m}\right) \eta_t e^{-\gamma(\sigma_e - \sigma_0)} \tag{6}$$

In addition, free gas stored within the effective pore-fracture volume is estimated according to the real-gas equation of state. The effective gas-filled volume can be expressed as:

$$Q_f = V_e \frac{\phi_f (1 - S_w) P}{\rho_c Z R T} \tag{7}$$

By combining the adsorbed-gas term and the free-gas term, the effective gas production potential model for deep CBM reservoirs is obtained as:

$$Q = Q_a + Q_f = Q_L \left(1 + \ln \frac{k_f}{k_m}\right) \eta_t e^{-\gamma(\sigma_e - \sigma_0)} + V_e \frac{\phi_f (1 - S_w) P}{\rho_c Z R T} \tag{8}$$

where Q is the predicted productivity; Q_a is the effective adsorbed gas content; Q_f is the effective free gas content; k_f is the fracture permeability; k_m is the matrix permeability; σ_e is the effective stress; σ_0 is the critical closure stress; γ is the stress sensitivity coefficient; ϕ_f is the effective porosity for free gas; S_w is the water saturation; P is the formation pressure; Z is the gas compressibility factor; R is the universal gas constant; T is the formation temperature; ρ_c is the coal density; and V_e is the effective reservoir volume.

It should be noted that the above formulas have common limitations in their practical applications. Coal reservoirs exhibit strong heterogeneity and multiscale fracture systems, which often cause discrepancies between predicted results and field observations. Future advances in deep CBM exploration and development will increasingly rely on advanced analytical methods and data-driven technologies. Emerging high-pressure adsorption experiments, *in-situ* spectroscopy, and isotope-resolved gas analyses offer improved characterization of gas occurrence and migration behavior under deep reservoir conditions (Wu et al., 2025). Concurrently, integration of artificial intelligence with geological, geomechanical, and production data enables intelligent optimization of fracturing parameters and real-time prediction of reservoir responses (Yan et al., 2021; Mohamed and Mehana, 2025). Future research should further address hydraulic fracturing optimization under deep high-stress conditions, long-term productivity maintenance, and techno-economic evaluations of integrated deep CBM production and CCUS systems. These efforts will help improve the technical feasibility, economic competitiveness, and low-carbon development potential of deep CBM resources.

4.3 Comparison of current research

This subsection interprets recent findings in relation to earlier studies. It also identifies current limitations and implications for deep CBM research.

Research in this field primarily aims to clarify the geological controls on deep CBM occurrence mechanisms. Based on the genetic framework summarized by Moore (2012), this review extends the discussion of CBM genetic models from shallow formations to deep formations. Evidence of microbial activity and alkane origins from representative cases, including the Bowen and Ordos basins, further demonstrates the viability of microbial processes in deep coal seams (Huang et al., 2017; Chen et al., 2023). Chemical reaction pathways and R_o ranges related to thermogenic processes were also synthesized. This synthesis improves the accuracy and applicability of hydrocarbon generation window classification (Moore, 2012; Liu et al., 2022). Critical depth classification for deep CBM, as proposed by Qin and colleagues in China, was further reviewed. To overcome the limitations of traditional depth-based methods, additional parameters were incorporated, including temperature, pressure, stress, coal strength, and maturity evolution. The coupling mechanisms between coal reservoir properties and stress regimes were also clarified (Qin et al., 2018; Li et al., 2023). In addition, multiscale mass transfer mechanisms and productivity evaluation models for deep CBM were examined. These analyses help bridge the gap between theoretical understanding and practical development strategies (Wang et al., 2023; Mohamed and Mehana, 2025).

On this basis, this review proposed several future research directions and emphasized the continuous refinement of theoretical frameworks. Further comprehensive studies are needed to generate robust evidence, correct existing biases, and formulate effective strategies. These efforts can promote stronger synergy between deep CBM mechanism research and field development practices.

5. Conclusions

This review systematically examined the occurrence mechanisms of deep CBM. First, deep CBM is dominated by thermogenic gas with supplementary biogenic contributions. The generation and evolution of multiphase hydrocarbons are largely controlled by coalification and organic matter maturation. Second, deep coal reservoirs under "three-high" geological conditions exhibit low porosity and permeability, strong CH_4 adsorption capacity, and a high proportion of free gas, implying a transitional gas storage state between adsorption and free accumulation. Third, tectonic structures and stress field evolution jointly control fracture system effectiveness, thereby influencing gas migration and enrichment. Fourth, a predictive formula for critical depth was developed by integrating multiple geological parameters based on existing theories. Finally, a coupled dual-field equation for matrix diffusion and fracture seepage was established, along with a modified productivity evaluation formula tailored to deep CBM.

This review focused on deep CBM occurrence mechanisms. Although deep CBM resources are abundant, their exploration and development remain challenging because of their substantial burial depths and complex geological conditions. The case analyses presented in this review demonstrate that sedimentary evolution, burial depth, tectonic activity, and lithological assemblages jointly control deep CBM generation, occurrence, and accumulation. Heterogeneity and multiscale fracture development in deep coal reservoirs may also introduce uncertainties in the application of the predictive equations proposed herein.

Overall, this review summarizes the current understanding of the mechanisms governing deep CBM occurrence and provides a conceptual basis for future investigations. Continued research on deep coal reservoirs will further improve our understanding of gas occurrence, migration, and enrichment processes. Such research will also promote the responsible utilization of deep CBM resources and support broader carbon emission reduction and low-carbon energy transition goals.

Acknowledgements

Thanks to the Xinjiang Key Laboratory for Geodynamic Processes and Metallogenic Prognosis of the Central Asian Orogenic Belt for providing the research platform. We thank Cheng Dong, Ziqiang Lin, Gencheng He, and Hang Li for their help in data analysis. This study was supported by Key Research and Development Program of Xinjiang Uygur Autonomous Region (Nos. 2024B01017-2 and 2024B03002), Tianshan Talent Training Program of Xinjiang Uygur Autonomous Region (No. 2023TSYCCX0006), National Natural Science Foundation of China (No. 42462019), and National Major Science and Technology Project of China (No. 2024ZD1406000). We would like to thank MJEditor (www.mjeditor.com) for its linguistic assistance during the preparation of this manuscript. Thanks are also extended to Advances in Geo-Energy Research Editor Prof. Jianchao Cai and four anonymous reviewers for their constructive comments.

Supplementary file

https://doi.org/10.46690/ager.2026.07.06

Conflicts of interest

The authors declare no competing interest.

Open Access This article is distributed under the terms and conditions of the Creative Commons Attribution (CC BY-NC-ND) license, which permits unrestricted use, distribution, and reproduction in any medium, provided the original work is properly cited.

References

Ali Aghighi, M., Cui, T., Schöning, G., et al. Subsidence associated with dewatering and gas extraction from coal seams: Contribution of desorption-induced coal shrinkage. Journal of Hydrology, 2024, 637: 131355.

Anees, A., Zhang, H., Ashraf, U., et al. Sand-ratio distribution in an unconventional tight sandstone reservoir of Hangjinqi area, Ordos Basin: Acoustic impedance inversion-based reservoir quality prediction. Frontiers in Earth Science, 2022, 10: 1018105.

Asif, M., Wang, L., Naveen, P., et al. Influence of competitive adsorption, diffusion, and dispersion of CH_4 and CO_2 gases during the CO_2-ECBM process. Fuel, 2024, 358: 130065.

Asif, M., Wang, L., Panigrahi, D. C., et al. Integrated assessment of CO_2-ECBM potential in Jharia Coalfield, India. Scientific Reports, 2022, 12(1): 7533.

Asmussen, P., Pidgeon, B., Gaede, O., et al. Deciphering a cryptic unconformity in the Surat Basin using high frequency detrital zircon U-Pb geochronology: Insights into basin dynamics on the north-east margin of Gondwana. Gondwana Research, 2023, 118: 117-134.

Bannerjee, M., Mendhe, V. A., Kamble, A. D., et al. Facets of coalbed methane reservoir in East Bokaro Basin, India. Journal of Petroleum Science and Engineering, 2022, 208: 109255.

Bao, Y., Wei, C., Wang, C., et al. Geochemical characteristics and generation process of mixed biogenic and thermogenic coalbed methane in Luling coalfield, China. Energy & Fuels, 2014, 28(7): 4392-4401.

Brakel, A. T., Totterdell, J. M., Wells, A. T., et al. Sequence stratigraphy and fill history of the Bowen Basin, Queensland. Australian Journal of Earth Sciences, 2009, 56(3): 401-432.

Bustin, A. M. M., Bustin, R. M., Chikatamarla, L., et al. Learnings from a failed nitrogen enhanced coalbed methane pilot: Piceance Basin, Colorado. International Journal of Coal Geology, 2016, 165: 64-75.

Cao, A., Jing, G., Dou, L., et al. Statistical analysis of distribution patterns of coal seams in fold zones in Northwest China. International Journal of Mining Science and Technology, 2018, 28(5): 819-828.

Cao, Z., Lin, B., Liu, T. The impact of depositional environment and tectonic evolution on coalbed methane occurrence in West Henan, China. International Journal of Mining Science and Technology, 2019, 29(2): 297-305.

Chelgani, S. C., Hower, J. C., Mastalerz, M., et al. Anomalies in Vicker's microhardness of subbituminous and high volatile bituminous coals. International Journal of Coal Geology, 2024, 296: 104659.

Chen, R., Bao, Y., Zhang, Y. A review of biogenic coalbed methane experimental studies in China. Microorganisms, 2023, 11(2): 304.

Chen, S., Tang, D., Tao, S., et al. *In-situ* stress measurements and stress distribution characteristics of coal reservoirs in major coalfields in China: Implication for coalbed methane (CBM) development. International Journal of Coal Geology, 2017, 182: 66-84.

Coe, H. H., Birgenheier, L. P., Fernandez, D. P., et al. Rare earth element enrichment in coal and coal-adjacent strata of the Uinta Region, Utah and Colorado. Frontiers in Earth Science, 2024, 12: 1381152.

Cui, T., Schoning, G., Gallagher, M., et al. A Coupled Hydro-Mechanical Modeling Framework to Concurrently Simulate Coal Seam Gas Induced Subsidence and Groundwater Impacts. Water Resources Research, 2025, 61: e2024WR039280.

Cumella, S. P., Scheevel, J. The Influence of Stratigraphy and Rock Mechanics on Mesaverde Gas Distribution, Piceance Basin, Colorado, in Understanding, Exploring, and Developing Tight-gas Sands, edited by S. P. Cumella, K. W. Shanley, and W. K. Camp, AAPG, Tulsa, Oklahoma, 2008.

Davydov, V. I. Tunguska coals, Siberian sills and the Permian-Triassic extinction. Earth-Science Reviews, 2021, 212: 103438.

Dunlop, E. C., Warner, D. S., Warner, P. E. R., et al. Ultra-deep Permian coal gas reservoirs of the Cooper Basin: Insights from new studies. The APPEA Journal, 2017, 57(1): 218-262.

Eberle, J., Cohen, J., Foster, J., et al. A new Late Cretaceous metatherian from the Williams Fork Formation, Colorado. PLOS One, 2024, 19(10): e0310948.

Everts, A. J. W., Alessio, L. D., Connell, C. J. Subsurface high-grading potential in coal seam gas in eastern Australia. Australian Journal of Earth Sciences, 2024, 71(1): 31-51.

Fall, A., Eichhubl, P., Cumella, S. P., et al. Testing the basin-centered gas accumulation model using fluid inclusion observations: Southern Piceance Basin, Colorado. AAPG Bulletin, 2012, 96(12): 2297-2318.

Freij-Ayoub, R. Opportunities and challenges to coal bed methane production in Australia. Journal of Petroleum Science and Engineering, 2012, 88-89: 1-4.

Fu, J., Li, B., Ren, C., et al. Study on Elastoplastic Damage Constitutive Model and Permeability Evolution Law of Gas-Bearing Coal. Rock Mechanics and Rock Engineering, 2024, 57(11): 9183-9205.

Ghosh, S., Ojha, A., Varma, A. K. Geochemical signatures of potassium metasomatism in anthracite from the Himalayan fold-thrust belts of Sikkim, India. International Journal of Coal Science & Technology, 2022, 9(1): 29.

Glatz, G., Alafnan, S., Gholami, R., et al. Effect of kerogen maturity on the adsorption capacity of CO_2 and CH_4: A molecular investigation. Fuel, 2022, 327: 125188.

Godec, M., Koperna, G., Gale, J. CO_2-ECBM: A review of its status and global potential. Energy Procedia, 2014, 63: 5858-5869.

Golding, S. D., Baublys, K. A., Glikson, M., et al. Source and Timing of Coal Seam Gas Generation in Bowen Basin Coals, in Coalbed Methane: Scientific, Environmental and Economic Evaluation, edited by M. Mastalerz, M. Glikson, and S.D. Golding, Springer, Dordrecht, pp. 257-269, 1999.

Govindarajan, S. K., Pavan, T. N. V., Devarapu, S. R., et al. Critical review on challenges in the application of Darcy's law for multi-phase fluid flow in petroleum reservoirs. Discover Applied Sciences, 2025, 7(3): 201.

Guang, W., Liu, X., Zhang, Z., et al. Nano-confinement effect on multi-mechanistic CO_2-CH_4 transport in coal: Upscaling from molecular dynamics to core experiments. Gas Science and Engineering, 2026, 149: 205885.

Hamilton, S. K., Golding, S. D., Esterle, J. S., et al. Controls on gas domains and production behaviour in a high-rank CSG reservoir: Insights from molecular and isotopic chemistry of co-produced waters and gases from the Bowen Basin, Australia. Geosciences, 2020, 10(2): 74.

Hazra, B., Wood, D. A., Panda, M., et al. Pore structural complexities and gas storage capacity of Indian coals with various thermal maturities. Energy & Fuels, 2025, 39(12): 5818-5831.

He, Y., Li, X., Cai, J., et al. Study of key factors for efficient coalbed methane extraction: Pore structure, desorption rate and seepage characteristics. Langmuir, 2025, 41(9): 6020-6036.

He, Z., Hu, Z., Nie, H., et al. Characterization of shale gas enrichment in the Wufeng Formation-Longmaxi Formation in the Sichuan Basin of China and evaluation of its geological construction-transformation evolution sequence. Journal of Natural Gas Geoscience, 2017, 2(1): 1-10.

Huang, J., Zhai, C., Sun, Y., et al. Nanoconfined methane recovery enhancement in deep coal seams via flue gas thermal stimulation: Molecular-level insights from realistic macromolecular models. Fuel, 2026, 404: 136157.

Huang, W., Li, J., Liu, Z., et al. Study of a low-disturbance pressure-preserving corer and its coring performance in deep coal mining conditions. International Journal of Mining Science and Technology, 2023, 33(11): 1397-1410.

Huang, Z., Sednek, C., Urynowicz, M. A., et al. Low carbon renewable natural gas production from coalbeds and implications for carbon capture and storage. Nature Communications, 2017, 8(1): 568.

Hu, H., Liu, S., Li, Z., et al. Pore and chemical structural evolution of coals with different ranks induced by supercritical CO_2: Combined experimental and multi-scale simulation study. Geoenergy Science and Engineering, 2026, 265: 214600.

Inagaki, F., Hinrichs, K. U., Kubo, Y., et al. Exploring deep microbial life in coal-bearing sediment down to 2.5 km below the ocean floor. Science, 2015, 349: 420-424.

Jiang, K., Ashworth, P. The development of Carbon Capture Utilization and Storage (CCUS) research in China: A bibliometric perspective. Renewable and Sustainable Energy Reviews, 2021, 138: 110521.

Jiang, L., Chen, Z., Farouq Ali, S. M., et al. Storing carbon dioxide in deep unmineable coal seams for centuries following underground coal gasification. Journal of Cleaner Production, 2022, 378: 134565.

Ji, Y., Li, S., Hou, W., et al. Influence of pore space of deep coal reservoirs on gas occurrence: A case study of Daning-Jixian area. International Journal of Hydrogen Energy, 2026, 227: 154388.

Johnson, R. C. Geologic history and hydrocarbon potential of Late Cretaceous-age, low-permeability reservoirs, Piceance Basin, western Colorado. Washington, D.C., USA, US Government Printing Office, 1989.

Johnson, R. C., Flores, R. M. Developmental geology of coalbed methane from shallow to deep in Rocky Mountain basins and in Cook Inlet - Matanuska basin, Alaska, U.S.A. and Canada. International Journal of Coal Geology, 1998, 35(1-4): 241-282.

Ju, W., Dong, J., Chang, C. Evolution of methane permeability and fracture structure of coal: Implications for methane extraction in deep coal seams. RSC Advances, 2022, 12(47): 30227-30235.

Ju, W., Shen, J., Qin, Y., et al. *In-situ* stress distribution and coalbed methane reservoir permeability in the Linxing area, eastern Ordos Basin, China. Frontiers of Earth Science, 2018, 12(3): 545-554.

Kang, H., Gao, F., Xu, G., et al. Mechanical behaviors of coal measures and ground control technologies for China's deep coal mines - A review. Journal of Rock Mechanics and Geotechnical Engineering, 2023, 15(1): 37-65.

Kędzior, S., Teper, L. Coal properties and coalbed methane potential in the southern part of the Upper Silesian Coal Basin, Poland. Energies, 2023, 16(7): 3219.

Kędzior, S., Teper, L. Occurrence and potential for coalbed methane extraction in the depocenter area of the Upper Silesian coal Basin (Poland) in the context of selected geological factors. Energies, 2024, 17(11): 2592.

Langmuir, I. The Adsorption of Gases on Plane Surfaces of Glass, Mica and Platinum. Journal of the American Chemical Society, 1918, 40(9): 1361-1403.

Lee, H., Muirhead, J. D., Fischer, T. P., et al. Massive and prolonged deep carbon emissions associated with continental rifting. Nature Geoscience, 2016, 9(2): 145-149.

Li, G., Jia, C., Zhao, Q., et al. Coal-rock gas accumulation mechanism and the whole petroleum system of coal measures. Petroleum Exploration and Development, 2025, 52(1): 33-49.

Li, G., Wang, G., Feng, N., et al. Deep coal-rock gas in China: A review of distribution, geological characteristics, and its enrichment conditions. ACS Omega, 2025, 10(22): 23472-23491.

Li, S., Qin, Y., Tang, D., et al. A comprehensive review of deep coalbed methane and recent developments in China. International Journal of Coal Geology, 2023, 279: 104369.

Li, S., Shao, L., Liu, J., et al. Oil generation model of the liptinite-rich coals: Palaeogene in the Xihu Sag, East China Sea Shelf Basin. Journal of Petroleum Science and Engineering, 2022, 209: 109844.

Li, S., Tang, D., Pan, Z., et al. Geological conditions of deep coalbed methane in the eastern margin of the Ordos Basin, China: Implications for coalbed methane development. Journal of Natural Gas Science and Engineering, 2018, 53: 394-402.

Li, Y., Zhai, C., Zhang, L., et al. Full-field experimental investigation of heat transfer and thermoelastic response during steam injection into coal seam borehole. Advances in Geo-Energy Research, 2026, 20(1): 27-42.

Li, Z., Li, S., Yu, X., et al. Coal bed methane enrichment regularities and controlling factors in Bowen-Surat basin, Australia. Coal Geology & Exploration, 2014, 42(6): 29-33. (in Chinese)

Li, Z., Zeng, Q., Xu, M., et al. Peat formation and accumulation mechanism in northern marginal basin of South China Sea. Acta Oceanologica Sinica, 2021, 40(2): 95-106.

Liu, C., Yang, Z., Qin, Y., et al. Excess pore pressure behavior and evolution in deep coalbed methane reservoirs. International Journal of Mining Science and Technology, 2024, 34(6): 763-781.

Liu, D., Jia, Q., Cai, Y., et al. A new insight into coalbed methane occurrence and accumulation in the Qinshui Basin, China. Gondwana Research, 2022, 111: 280-297.

Liu, S., Wang, H., Sang, S., et al. Effects of pore structure changes on the CH_4 adsorption capacity of coal during CO_2-ECBM. Fuel, 2022, 330: 125529.

Longinos, S. N., Begaliyev, D., Asif, M., et al. Cryogenic fracturing of coal with LN_2 treatment: A sustainable approach for enhancing coalbed methane extraction in water-scarce regions. Gas Science and Engineering, 2025, 142: 205686.

Lu, B., Yang, Z., Hou, Y., et al. Desorption-diffusion specificity of deep coalbed methane under high-temperature effects: Implications for development. International Journal of Mining Science and Technology, 2025, 35(9): 1511-1527.

Lu, Y., Han, J., Zhang, H., et al. Study on coal seam physical characteristics and influence on stimulation: A case study of coal seams in Zhengzhuang Block. Frontiers in Earth Science, 2023, 10: 1031419.

Lv, D., Song, Y., Shi, L., et al. The complex transgression and regression history of the northern margin of the Palaeogene Tarim Sea (NW China), and implications for potential hydrocarbon occurrences. Marine and Petroleum Geology, 2020, 112: 104041.

Lv, F., Yang, R., Gao, W., et al. Critical depth prediction based on *in-situ* stress and gas content model of deep coalbed methane in Liupanshui Coalfield in China. Scientific Reports, 2025, 15(1): 297.

Masum, S. A., Sadasivam, S., Chen, M., et al. Low subcritical CO_2 adsorption-desorption behavior of intact bituminous coal cores extracted from a shallow coal seam. Langmuir, 2023, 39(4): 1548-1561.

Mohamed, T., Mehana, M. Coalbed methane characterization and modeling: Review and outlook. Energy Sources Part A: Recovery Utilization and Environmental Effects, 2025, 47(1): 2874-2896.

Mohanty, M. M., Pal, B. K. Sorption behavior of coal for implication in coal bed methane an overview. International Journal of Mining Science and Technology, 2017, 27: 307-314.

Moore, T. A. Coalbed methane: A review. International Journal of Coal Geology, 2012, 101: 36-81.

Mostafa, A., Scholtès, L., Golfier, F. Pore-scale hydromechanical modeling of gas transport in coal matrix. Fuel, 2023, 345: 128165.

Mudoi, M. P., Sharma, P., Khichi, A. S. A review of gas adsorption on shale and the influencing factors of CH_4 and CO_2 adsorption. Journal of Petroleum Science and Engineering, 2022, 217: 110897.

Mukherjee, M., Misra, S. A review of experimental research on Enhanced Coal Bed Methane (ECBM) recovery via CO_2 sequestration. Earth-Science Reviews, 2018, 179: 392-410.

Mwakipunda, G. C., Wang, Y., Mgimba, M. M., et al. Recent Advances in Carbon Dioxide Sequestration in Deep Unmineable Coal Seams Using CO_2 -ECBM Technology: Experimental Studies, Simulation, and Field Applications. Energy & Fuels, 2023, 37(22): 17161-17186.

Oremland, R. S., Polcin, S. Methanogenesis and sulfate reduction: Competitive and noncompetitive substrates in estuarine sediments. Applied and Environmental Microbiology, 1982, 44(6): 1270-1276.

Pajdak, A., Kudasik, M., Skoczylas, N., et al. Studies on the competitive sorption of CO_2 and CH_4 on hard coal. International Journal of Greenhouse Gas Control, 2019, 90: 102789.

Pandey, S., Flook, S., Cox, R., et al. Underground water impact report 2021 for the Surat cumulative management area. Brisbane, Department of Regional Development, Manufacturing and Water, 2021.

Pang, X., Jia, C., Chen, J., et al. A unified model for the formation and distribution of both conventional and unconventional hydrocarbon reservoirs. Geoscience Frontiers, 2021, 12(2): 695-711.

Panwar, D. S., Suman, S., Singh, A. K., et al. Assessment of hydrocarbon generation potential of bituminous coal from Raniganj Basin, India. Energy Sources, Part A: Recovery, Utilization, and Environmental Effects, 2020, 42(7): 824-834.

Pedersen, K. Exploration of deep intraterrestrial microbial life: Current perspectives. Fems Microbiology Letters, 2000, 185(1): 9-16.

Perera, M. A comprehensive overview of CO_2 flow behaviour in deep coal seams. Energies, 2018, 11(4): 906.

Qin, Y., Moore, T. A., Shen, J., et al. Resources and geology of coalbed methane in China: A review. International Geology Review, 2018, 60(5-6): 777-812.

Rafiei Renani, H., Cai, M. Forty-year review of the Hoek-Brown failure criterion for jointed rock masses. Rock Mechanics and Rock Engineering, 2022, 55(1): 439-461.

Rajabi, M., Ziegler, M., Heidbach, O., et al. Contribution of mine borehole data toward high-resolution stress mapping: An example from northern Bowen Basin, Australia. International Journal of Rock Mechanics and Mining Sciences, 2024, 173: 105630.

Ren, Y., Yuan, Q., Jiang, D., et al. A non-Darcy gas flow model for coalbed methane in mine gobs. Physics of Fluids, 2021, 33(11): 116601.

Sahlström, F., Dirks, P., Chang, Z., et al. The Paleozoic Mount Carlton deposit, Bowen basin, northeast Australia: Shallow high-sulfidation epithermal Au-Ag-Cu mineralization formed during rifting. Economic Geology, 2018, 113(8): 1733-1767.

Salmachi, A., Rajabi, M., Wainman, C., et al. History, geology, in situ stress pattern, gas content and permeability of coal seam gas basins in Australia: A review. Energies, 2021, 14(9): 2651.

Sampath, K. H. S. M., Perera, M. S. A., Ranjith, P. G., et al. CH_4-CO_2 gas exchange and supercritical CO_2 based hydraulic fracturing as CBM production-accelerating techniques: A review. Journal of CO_2 Utilization, 2017, 22: 212-230.

Scott, A. R., Kaiser, W. R., Ayers Jr, W. B. Thermogenic and Secondary Biogenic Gases, San Juan Basin, Colorado and New Mexico — Implications for Coalbed Gas Producibility. AAPG Bulletin, 1994, 78(8): 1186-1209.

Song, J., Liu, C., Liu, Y. Mechanism of coalbed methane migration and production based on micro-pore overpressure environment. Petroleum Science and Technology, 2022, 40(24): 2971-2987.

Song, Y., Liu, S., Zhang, Q., et al. Coalbed methane genesis, occurrence and accumulation in China. Petroleum Science, 2012, 9(3): 269-280.

Sosnowski, P., Jelonek, I. Facies development of coal seams in the Knurów deposit (Upper Silesia, Poland). International Journal of Coal Geology, 2022, 261: 104073.

Stroker, T. M., Harris, N. B., Crawford Elliott, W., et al. Diagenesis of a tight gas sand reservoir: Upper Cretaceous Mesaverde Group, Piceance Basin, Colorado. Marine and Petroleum Geology, 2013, 40: 48-68.

Tamamura, S., Murakami, T., Ueno, A., et al. Formation of

coalbed methane and water-dissolved gas in Kushiro Coal Mine, Japan, based on isotopic compositions of gas, groundwater, and calcite. International Journal of Coal Geology, 2020, 229: 103577.
Tambaria, T. N., Sugai, Y., Nguele, R. Adsorption factors in enhanced coal bed methane recovery: A review. Gases, 2022, 2(1): 1-21.
Tian, F., Liang, Y., Wang, D., et al. Effects of caprock sealing capacities on coalbed methane preservation: Experimental investigation and case study. Journal of Central South University, 2019, 26: 925-937.
Tonnsen, R. R., Miskimins, J. L. Simulation of deep coalbed methane permeability and production assuming variable pore volume compressibility. Paper SPE 138160 Presented at SPE Canadian Unconventional Resources and International Petroleum Conference, Calgary, Alberta, Canada, 19-21 October, 2010.
Towler, B., Firouzi, M., Underschultz, J., et al. An overview of the coal seam gas developments in Queensland. Journal of Natural Gas Science and Engineering, 2016, 31: 249-271.
Ullah, B., Cheng, Y., Wang, L., et al. Experimental analysis of pore structure and fractal characteristics of soft and hard coals with same coalification. International Journal of Coal Science & Technology, 2022, 9(1): 58.
Underschultz, J. R., Pasini, P., Grigorescu, M., et al. Assessing aquitard hydraulic performance from hydrocarbon migration indicators: Surat and Bowen basins, Australia. Marine and Petroleum Geology, 2016, 78: 712-727.
Vasilenko, T., Kirillov, A., Islamov, A., et al. Permeability of a coal seam with respect to fractal features of pore space of fossil coals. Fuel, 2022, 329: 125113.
Wadsworth, J., Boyd, R., Diessel, C., et al. Stratigraphic style of coal and non-marine strata in a tectonically influenced intermediate accommodation setting; the Mannville Group of the Western Canadian Sedimentary Basin, south-central Alberta. Bulletin of Canadian Petroleum Geology, 2002, 50: 507-541.
Wang, Q., Ji, M., Liu, G., et al. Multi-field coupled mathematical modeling and numerical simulation technique of gas transport in deep coal seams. Advances in Geo-Energy Research, 2025, 15(1): 87-90.
Wang, T., Fan, W., Lin, H., et al. Micropore structure characteristics and gas-bearing properties of deep coal reservoirs: A case study of the Benxi Formation in the Daning-Jixian Block. Energy Geoscience, 2026, 7(5): 100581.
Wang, T., Tian, F., Deng, Z., et al. The characteristic development of micropores in deep coal and its relationship with adsorption capacity on the eastern margin of the Ordos Basin, China. Minerals, 2023, 13(3): 302.
Wang, T., Zhou, G., Fan, L., et al. Full-scale pore and microfracture characterization of deep coal reservoirs: A case study of the Benxi Formation coal in the Daning-Jixian Block, China. International Journal of Energy Research, 2024, 2024(1): 5772264.
Wang, Y., Yu, H., Jia, Z., et al. Transient pressure analysis of polymer flooding fractured wells with oil-water two-phase flow. Petroleum Exploration and Development, 2023, 50(1): 175-182.
Wang, Z., Liu, S., Qin, Y. Coal wettability in coalbed methane production: A critical review. Fuel, 2021, 303: 121277.
Wei, Q., Li, X., Zhang, J., et al. Full-size pore structure characterization of deep-buried coals and its impact on methane adsorption capacity: A case study of the Shihezi Formation coals from the Panji Deep Area in Huainan Coalfield, Southern North China. Journal of Petroleum Science and Engineering, 2019, 173: 975-989.
Welsby, D., Price, J., Pye, S., et al. Unextractable fossil fuels in a 1.5 °C world. Nature, 2021, 597: 230-234.
Wen, Z., Guo, S., Zhao, Y., et al. Mechanism of microscopic behind the influence of stress loading on gas adsorption by coal. Scientific Reports, 2025, 15(1): 3253.
Whelan, J. K., Farrington, J. W., Tarafa, M. E., et al. Maturity of organic matter and migration of hydrocarbons in two Alaskan North Slope wells. Organic Geochemistry, 1986, 10(1-3): 207-219.
Wood, J. M., Sanei, H. Secondary migration and leakage of methane from a major tight-gas system. Nature Communications, 2016, 7(1): 13614.
Wu, S., Tang, D., Li, S., et al. Coalbed methane adsorption behavior and its energy variation features under supercritical pressure and temperature conditions. Journal of Petroleum Science and Engineering, 2016, 146: 726-734.
Wu, X., Meng, Q., Zhu, H., et al. Adsorption-induced negative carbon isotope sequence in over-mature coal-type gas from the southwest Ordos Basin. Scientific Reports, 2025, 15(1): 12048.
Xiao, Z., Wang, G., Liu, J., et al. Experimental study and model improvement on coal permeability: The influence of effective stress, slip effect, and water content. International Journal of Rock Mechanics and Mining Sciences, 2025, 185: 105972.
Xu, F., Hou, W., Xiong, X., et al. The status and development strategy of coalbed methane industry in China. Petroleum Exploration and Development, 2023, 50(4): 765-783.
Yang, W., Bai, Y., Sun, X., et al. The influence of hydrocarbon generation on the sealing capability of mudstone caprock rich in organic matter. Scientific Reports, 2024, 14(1): 1846.
Yang, Y., Liu, S., Zhao, W., et al. Intrinsic relationship between Langmuir sorption volume and pressure for coal: Experimental and thermodynamic modeling study. Fuel, 2019, 241: 105-117.
Yang, Y., Xin, H., Zhang, P., et al. Study on the microscopic mechanism of competitive adsorption and swelling-diffusion effects of CO_2/CH_4 in coal under the influence of organic micromolecules. Chemical Engineering Science, 2026, 324: 123326.
Yan, T., He, S., Zheng, S., et al. Critical tectonic events and their geological controls on deep buried coalbed methane accumulation in Daning-Jixian Block, eastern Ordos Basin. Frontiers of Earth Science, 2023, 17(1): 197-217.
Yan, Y., Borhani, T. N., Subraveti, S. G., et al. Harnessing the power of machine learning for carbon capture, utilisation, and storage (CCUS) - A state-of-the-art review. Energy

& Environmental Science, 2021, 14(12): 6122-6157.

Yao, W., Zhao, H., Li, P., et al. Stress-release-induced evolution of pore-fracture morphology and connectivity in deep coal seams: A case study of the Daning-Jixian block. Theoretical and Applied Mechanics Letters, 2026, 100697.

Zhang, B., Tao, S., Yang, F., et al. The genesis and accumulation mechanism of CBM in the typical mid- to low-rank coal-bearing basins. Petroleum Science, 2025, 22(8): 3069-3085.

Zhang, J., Li, G., Jia, C., et al. Natural gas types and coal-rock gas classification in the whole petroleum system of coal measures. Petroleum Exploration and Development, 2025, 52(4): 894-906.

Zhao, S., Wei, S., Zhang, L., et al. Dynamic mechanical response and crack evolution law of raw coal loaded by dynamic-static coupling under three-dimensional constraints. Scientific Reports, 2024, 14(1): 8659.

Zhao, Z., Xu, W., Zhao, Z., et al. Geological characteristics and exploration breakthroughs of coal rock gas in Carboniferous Benxi Formation, Ordos Basin, NW China. Petroleum Exploration and Development, 2024, 51(2): 262-278.

Zheng, G., Sun, B., Lv, D., et al. Study on reservoir properties and critical depth in deep coal seams in Qinshui Basin, China. Advances in Civil Engineering, 2019, 2019: 1683413.

Zhou, H., Rong, T., Wang, L., et al. A new anisotropic coal permeability model under the influence of stress, gas sorption and temperature: Development and verification. International Journal of Rock Mechanics and Mining Sciences, 2020, 132: 104407.

Zou, G., Zhang, Q., Peng, S., et al. Influence of geological factors on coal permeability in the Sihe coal mine. International Journal of Coal Science & Technology, 2022, 9(1): 6.

Zou, Y., Kang, Y., Chen, M., et al. Multiscale insights into CH_4/CO_2 desorption-diffusion under thermal-pressure-moisture coupling in deep coalbed methane nano-confined. Chemical Engineering Science, 2026, 320: 122506.